First Results of AC Loss Test on ITER TF Conductors With Transverse Load Cycling

Y. Miyoshi, G. Rolando, A. Vostner, Y. Nabara, and A. Nijhuis

***Abstract*—The influence of the expected Lorentz loading and time dependent operating conditions of a magnet on the conductor AC loss is experimentally simulated by a cryogenic cable press that applies cyclic mechanical loading. A series of ITER conductor tests with the press have commenced and we report on the results from the first set of two TF conductors, which have the option-II cabling scheme but consist of Nb_3Sn strands from different manufacturers. With the press, we apply a transverse load of 578 kN/m and the load cycle is repeated up to 30,000 times. As a function of load cycles, we measure the cable mechanical stiffness, interstrand contact resistances, and the coupling loss. When compared with a previously measured option-II type conductor, the present conductors have higher initial losses. However, they showed greater cable displacement and larger increase in contact resistance with load cycles. This is due to the lower cable stiffness thought to be related to the lower axial strand stiffness, resulting in greater cable displacement than the previous cable. Consequently, the two conductors tested here have lower losses already within the first few cycles.**

***Index Terms*—CICC, contact resistance, coupling loss, transverse load.**

I. Introduction

THE CYCLIC Lorentz force loading under ITER cable-in-conduit conductor (CICC) operating conditions induces plastic deformation of superconducting strands and strand movements that result in degradation of transport performance as well as in changes of the cable coupling loss. The cable coupling loss is a function of inductive coupling between each strand segment with every other strand segments [1] in the cable, and it is determined by the interstrand contact resistance, R_c, and the cabling twist pitches. The cable deformation and R_c, therefore, are important parameters in understanding the evolution of cable coupling loss with load cycles.

The Twente cable press facility measures the R_c, the cable mechanical properties, and the AC loss as a function of transverse load cycles at cryogenic temperature [2]–[5]. The recent measurement of a conductor with option-II cabling scheme showed contrasting behavior compared to the prototypes as a consequence of the longer twist pitches. The longer pitches resulted in higher initial coupling loss time constant $n\tau$, and in greater strand movement so that the loss time constant reduced to about 200 ms within the first 100 cycles.

A series of tests with the press have commenced as a part of ITER conductor characterization and we report the results from the first set of Toroidal Field (TF) conductors (referred to as TFJA5-A and TFJA5-B) which are option-II conductors. These results are compared with our previous measurement on EUTF3-EAS. We find that both TFJA5 conductors have a rather high $n\tau$, but also have smaller cable stiffness. A numerical model calculation of the loss with a measured R_c distribution as an input parameter are also presented.

II. Conductor Samples and Test Procedures

The full identities of the conductor samples tested are TFJA5-A (81JNC001-S4T1) and TFJA5-B (81JNC002-S4T1). The cable constituents are 900 Nb_3Sn strands produced by TFJA5-A and TFJA5-B, respectively, and 522 Cu strands. The nominal cabling pitches for an option-II cable are 80/140/190/300/420 mm and the void fraction is 29%. Their transport properties and the degradation with load cycles and also the AC loss have already been measured at the SULTAN test facility earlier [6].

The press measurement length of a cable specimen is 40 cm. Since a TF conductor has a round jacket, it is placed in a square dummy jacket to be inserted into the press. The cable jacket is cut in half with a separation of $\sim$7 mm so that the transverse load applied by the press will compress the cable itself. While cutting the jacket, the initial condition of the cable is maintained by clamping with the bolts both halves of the dummy jacket [4]. R_c measurements are performed only on the TFJA5-A cable and for this an extra 20 cm length of the cable is used for selecting strand combinations.

Our test procedure is as follows. The press applies a maximum load of 578 kN/m, which is equivalent to the expected peak load condition for a TF conductor, and the load/unload cycle is repeated up to 30,000 cycles. At selected load cycles we measure the AC loss, the cable compaction (jacket displacement), and R_c. At zero applied load and at full load, the cable AC loss is measured by a calibrated set of pick-up coils wound on the cable. The magnetizing field is a sinusoidal AC field between 0.2 and 0.5 T at a frequency range between 0.01 to 0.12 Hz produced by a superconducting dipole surrounding the sample chamber of the press. For the TFJA5-A conductor, R_c measurements are also performed by the standard four-point technique between a pair of strands selected from the first, second, third, and fourth intra-petal cabling stages and between different petals. Only the superconducting strand

Manuscript received September 13, 2011; accepted November 27, 2011. Date of publication December 05, 2011; date of current version May 24, 2012. This work was supported in part by the ITER International Organization under Contract ITER/CT/09/4300000059.

Y. Miyoshi, G. Rolando, and A. Nijhuis are with the Low Temperature Division, Faculty of Science and Technology, University of Twente, 7500AE Enschede, The Netherlands (e-mail: y.miyoshi@tnw.utwente.nl).

A. Vostner is with ITER Organization, Route de Vinon, 13115 St Paul lez Durance, France.

Y. Nabara is with ITER superconducting magnet technology group, Japan Atomic Energy Agency, 801-1 Mukoyama, Naka, Ibaraki 311-0193, Japan.

Digital Object Identifier 10.1109/TASC.2011.2178218

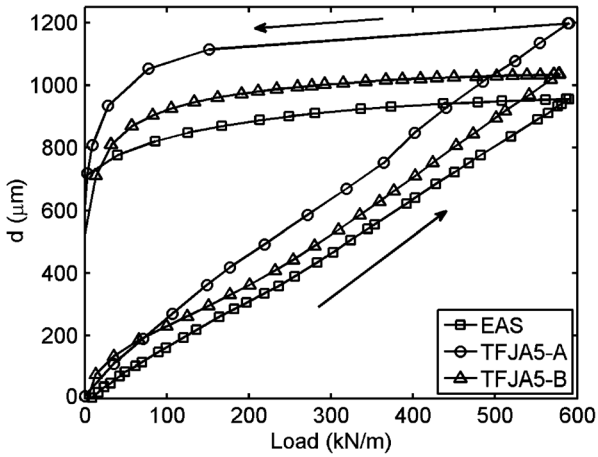

Fig. 1. Measured cable displacements at the first load/unload cycle for the three conductors. Arrows indicate the direction of load cycle.

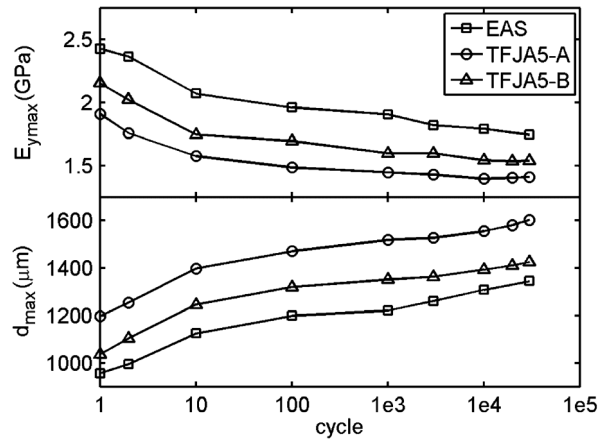

Fig. 2. Displacement (bottom) and Ey (top) measured at the full load.

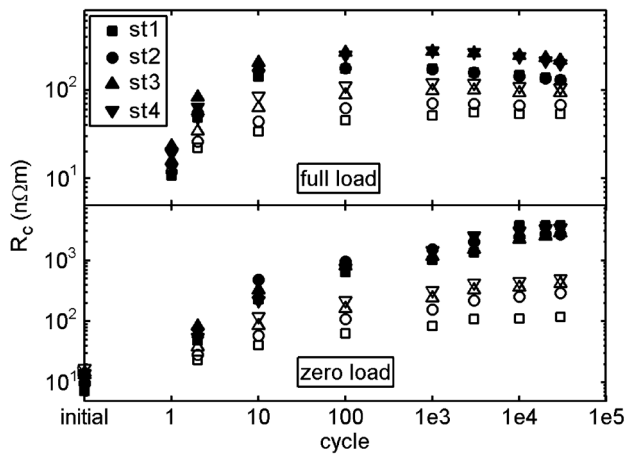

Fig. 3. R_c for intra-petal stage 1, 2, 3, and 4 for TFJA5-A (filled) and EAS (open) with cycles.

pairs are chosen. At each of the loading/unloading steps, the overall cable displacement is measured by six sets of calibrated extensometers, symmetrically mounted on each side of the conductor. At all time, the sample does not carry any transport current. Further details of the measurement technique can be found elsewhere [2], [4].

III. Cable Stiffness

The overall cable compaction, d, measured with respect to applied load at the first load cycle is shown in Fig. 1. The hysteretic displacement loop is a typical behavior of $\mathrm{Nb_3Sn}$ CICC. For comparison, previously measured result on the EUTF3-EAS sample (hereafter EAS) is also shown. In our previous analysis [5], EAS compared to the prototypes with short pitches had the greatest displacement with applied load, due to longer twist pitches resulting in loosely bound strands. Assuming that the three cables have the same cabling pitches and void fractions that do not deviate greatly from their nominal ones, the difference in the displacement can be associated with the difference in axial strand stiffness. In reality, small variations in cable properties, such as the strand diameter, the jacket inner diameter, the central spiral, and the cable twist pitches, may result in a small variation in void fraction that also has an impact on the cable stiffness. Nevertheless, the axial stress-strain tests on the strands [7], show EAS strand has the highest stiffness while TFJA5-B strand is slightly stiffer than TFJA5-A strand, which is qualitatively in agreement with the observed magnitude in cable displacement. The transverse cable stiffness is evaluated by

$$E_y = \frac{DF_y}{A_y d} \tag{1}$$

where D is the cable diameter, A_y is the average longitudinal cable cross section, and d is the cable displacement. The evolution of cable stiffness and the maximum cable displacement with cycles are shown in Fig. 2. The compaction history and the cable stiffness change with cycles are similar for the three cables and only the absolute values are different. The TFJA5-A cable has the smallest stiffness, and although we may not straightforwardly relate the cable stiffness to the transport degradation with cycles, we note that the TFJA5-A cable has the greatest T_{cs} degradation with the electromagnetic load cycles in SULTAN test [6].

IV. R_C Measurements

The initial triplet R_c for TFJA5-A is 7 $\mathrm{n\Omega m}$ which is slightly smaller than EAS which had 10 $\mathrm{n\Omega m}$. The initial mean value of all intra-petal R_c is 11 $\mathrm{n\Omega m}$ for TFJA5-A and 12 $\mathrm{n\Omega m}$ for EAS. Immediately after the first loading, the distribution of R_c becomes clearly different between the two conductors (Fig. 3). With load cycles, EAS has consistently lower R_c for all intra-petal cabling stages and its R_c distribution follows the cabling stage order. In contrast, the ordering in R_c for TFJA5-A becomes less clear already after the first load cycle. At the final cycle, the average intra-petal R_c for TFJA5-A is approximately an order of magnitude greater at zero load and about twice as great at full load than for EAS. In both conductors, intra-petal R_c increases with load cycles. The mechanism of increase in R_c is thought to be related with disengagement from the oxygen free contacts formed between Cr coated $\mathrm{Nb_3Sn}$ strands during the heat treatment [8]. We may assume that initially the two conductors have identical number of oxygen free contacts, and we speculate that the greater increase in R_c for the TFJA5-A conductor is associated with the stiffness of the conductor i.e., the degree of freedom for strand movements. Other factors such as

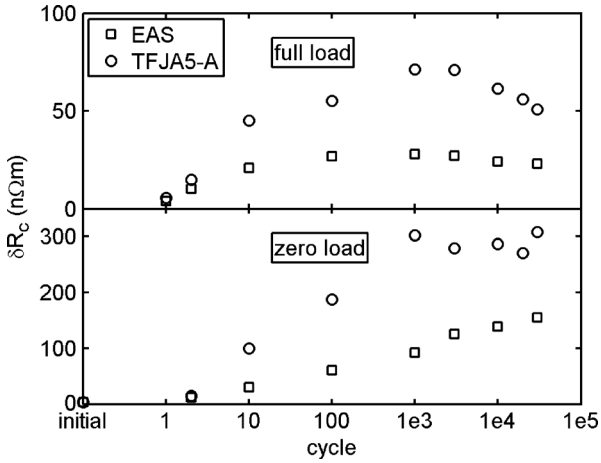

Fig. 4. Gaussian widths δR_c of cumulative frequency distribution for R_c.

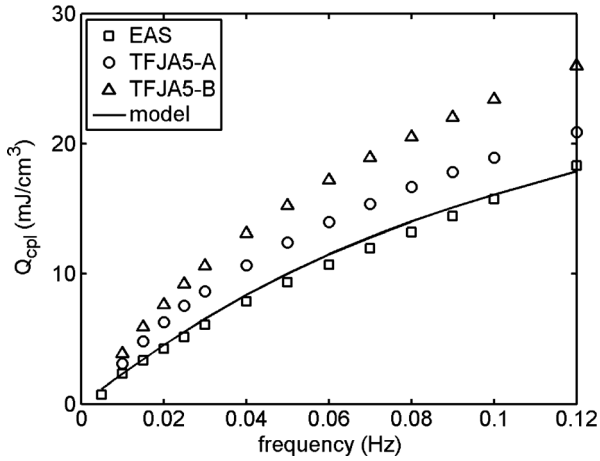

Fig. 5. The initial coupling loss measured for EAS, TFJA5-A and TFJA5-B conductors (symbols) and a computation by the numerical cable model with input R_c distribution from EAS (line).

the difference in Cr layer properties between Cr vendors [9] may also affect the behavior of R_c evolution. The Gaussian width δR_c of the cumulative frequency [10] for intra-petal R_c shows clearly that the spread in R_c is much greater in TFJA5-A (Fig. 4).

The evolution of inter-petal R_c with cycles for TFJA5-A is practically identical to that in EAS and it is thought that the current paths are determined mostly by the petal coverage with stainless steel wraps. The initial average inter-petal R_c for EAS is 96 $\mathrm{n\Omega m}$, which increases and saturates at final values of 4000 $\mathrm{n\Omega m}$ at zero load and at 260 $\mathrm{n\Omega m}$ at full load. For TFJA5-A, the initial value is 200 $\mathrm{n\Omega m}$ and the final values are 9200 $\mathrm{n\Omega m}$ (zero load) and 370 $\mathrm{n\Omega m}$ at full load. Although the overall trend is dictated by the presence of petal wraps, R_c is higher in TFJA5-A since intra-petal R_c is higher. The intra-petal R_c for TFJA5-A becomes so high with cycles that at the final cycle at zero load, it is only half of the average inter-petal R_c while for EAS intra-petal R_c is an order of magnitude smaller than inter-petal R_c at the final cycle at zero load.

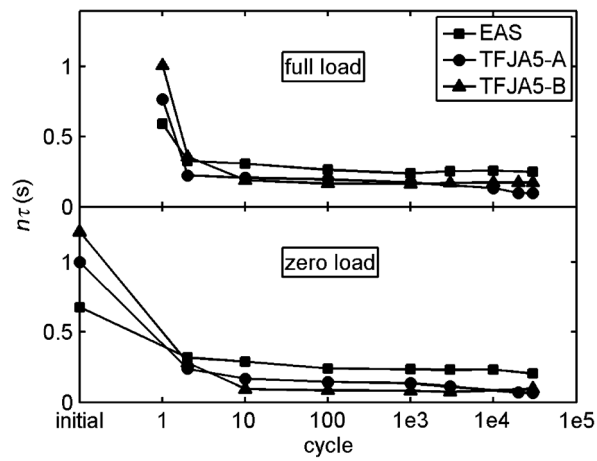

Fig. 6. Evolution of nt with load cycles measured at zero load (bottom) and at full load (top).

V. Coupling Loss vs Cyclic Loading

The measured AC loss is given per unit volume of superconducting strand in the cable and the coupling loss is evaluated by subtracting the hysteresis loss. A comparison of the initial coupling loss is shown in Fig. 5. Even though the initial R_c values are very similar for TFJA5-A and EAS, loss versus frequency curves are rather different. For TFJA5-A and TFJA5-B conductors, the losses we measure with the press are qualitatively in agreement with the losses at frequencies greater than 0.2 Hz measured at SULTAN. Due to the difference in the frequency range of magnetizing field, the field profile, the sample length, and the sample loading history, it is not possible to make a straightforward comparison with the SULTAN test results [11], and the agreement for EAS conductor is poor. Still, EAS has the lowest loss and TFJA5-B has the highest loss.

Recently, we have developed the numerical model JackPot to simulate the coupling loss of a CICC [1]. The model constructs the cable geometry by calculating the individual strand coordinates along their cable trajectories. The strand coordinates then determine the strand-to-strand distance and contact area. Once the cabling geometry is defined, the model takes the measured R_c distribution as an input parameter to calculate the contact resistivity which is a material property of strand-to-strand contact. The mutual inductance of each strand segment is calculated from the defined strand coordinates. A network of strands consisting of contact resistances and strand inductances is solved to calculate the coupling loss generated by external field. Here, we have simulated a case of option-II cabling geometry with the input R_c distribution measured from EAS (Fig. 5). The loss calculation is performed only for a single petal i.e., neglecting the inter-petal coupling, but it is in good agreement with the experiment. Since the initial R_c distribution is similar between TFJA5-A and EAS, the model is not able to reproduce the measured TFJA5-A loss curve. Therefore, we suspect the higher loss for TFJA5-A is due to variations in twist pitches.

We evaluate the coupling loss time constant $n\tau$ as a measure of loss by fitting the linear slope of loss curve in the low frequency limit [2]. The evolution of $n\tau$ with cycles is shown in Fig. 6. Initial $n\tau$ for TFJA5-A is 1000 ± 30 ms, for TFJA5-B is 1220 ± 30 ms, and for EAS 680 ± 40 ms. The initially high measured $n\tau$ for TFJA5-A and TFJA5-B decay much faster than for

EAS; already after the first cycle reduced to one quarter of the original values. Finally $n\tau$ saturate at 65 $\pm$ 3 ms for zero load and at 96 $\pm$ 5 ms for full load for TFJA5-A, and at 95 $\pm$ 10 ms for zero load and at 170 $\pm$ 10 ms for full load for TFJA5-B. In comparison, the final $n\tau$ values for EAS is 200 $\pm$ 10 ms for zero load and 250 $\pm$ 15 ms for full load. While $n\tau$ for TFJA5-A and TFJA5-B reduce to less than 10% of their initial values, $n\tau$ for EAS reduces to only $\sim$30% of the initial value. The decrease of $n\tau$ is partly reflected in the increase in intra-petal R_c and its distribution, and it is likely that the cable deformations also play a role. We will be investigating the initial and the final cabling geometries of the three conductors by using our JackPot cable model to simulate the evolution of $n\tau$.

VI. Summary

We have measured the intra-petal and inter-petal R_c distribution, the cable stiffness and deformation, and the coupling loss of both TFJA5 conductors as a function of cyclic transverse loading up to 30,000 cycles. Despite the same cabling scheme, the TFJA5-A and TFJA5-B conductors have an initial $n\tau$ of 1000 ms and 1220 ms, respectively, compared to 680 ms for the EAS conductor. In terms of cable stiffness, TFJA5-A is the softest and EAS is the stiffest which correlates well with the order of strand axial stiffness. With TFJA5-A being less stiff, we find much greater increase in R_c and R_c distribution with cycles that may suggest greater strand movements in the conductor although other explanations may be possible. Also, the greater decrease in $n\tau$ for TFJA5-A and TFJA5-B may be associated with the greater change in R_c. Inspection of the cabling patterns before and after the load cycles will be carried out and further work is ongoing with the numerical model to simulate the evolution of $n\tau$ with cycles.

References

[1] E. P. A. van Lanen and A. Nijhuis, "Simulation of interstrand coupling loss in cable-in-conduit conductors with JackPot AC," *IEEE Trans. Appl. Supercond.*, vol. 21, no. 3, pp. 1926–1929, 2011.

[2] A. Nijhuis, N. W. Noordman, H. H. J. ten Kate, N. Mitchell, and P. Bruzzone, "Electromangetic and mechanical characterization of ITER CS-MC conductors affected by transverse cyclic loading, part 1: Coupling current loss," *IEEE Trans. Appl. Supercond.*, vol. 9, no. 2, pp. 1069–1072, 1999.

[3] A. Nijhuis, Y. Ilyin, W. Abbas, H. H. J. ten Kate, M. V. Ricci, and A. della Corte, "Impact of void-fraction on mechanical properties and evolution of coupling loss in ITER Nb_3Sn conductors under cyclic loading," *IEEE Trans. Appl. Supercond.*, vol. 15, no. 2, pp. 1633–1636, 2005.

[4] A. Nijhuis and Y. Ilyin, "Transverse cable stiffness and mechanical losses associated with load cycles in ITER Nb_3Sn and NbTi CICCs," *Supercond. Sci. Technol.*, vol. 22, p. 055007, 2009.

[5] Y. Miyoshi, Y. Ilyin, W. Abbas, and A. Nijhuis, "AC loss, inter-strand resistance, and mechanical properties of an option-II ITER CICC up to 30,000 cycles in the press," *IEEE Trans. Appl. Supercond.*, vol. 21, no. 3, pp. 1944–1947, 2011.

[6] Y. Nabara *et al.*, "Examination of Japanese mass produced Nb_3Sn superconductors for ITER Toroidal Field coils," *IEEE Trans. Appl. Supercond.*, to be published.

[7] A. Nijhuis *et al.*, to be published.

[8] A. Nijhuis and H. H. J. ten Kate, "Surface oxidation and interstrand contact resistance of Cr-coated Nb3Sn and bare NbTi strands in CICC's," *Adv. Cryo. Eng. Mater.*, vol. 46b, pp. 1083–1089, 2000.

[9] P. Bruzzone, A. Nijhuis, and H. H. J. ten Kate, "Effect of Cr plating on the coupling current loss in cable-in-conduit conductors," in *Proc. ICEC16/ICMC*, 1997, vol. 2, pp. 1243–1248.

[10] E. P. A. van Lanen, L. Feng, R. P. Pompe van Meerdervoort, W. A. J. Wessel, and A. Nijhuis, "Interstrand resistance measurements on the conductor terminations of TFPRO2 and JATF3 SULTAN samples," *IEEE Trans. Appl. Supercond.*, vol. 20, no. 3, pp. 474–477, 2010.

[11] P. Bruzzone, B. Stepanov, and E. Zapretilina, "A critical review of coupling loss results for cable-in-conduit conductors," *IEEE Trans. Appl. Supercond.*, vol. 16, no. 2, pp. 827–830, 2006.